

Search for sterile neutrino oscillation using RENO and NEOS data

Z. Atif,¹ J. H. Choi,² H. I. Jang,³ J. S. Jang,⁴ S. H. Jeon,⁵ K. K. Joo,¹ K. Ju,⁶ D. E. Jung,⁵ J. G. Kim,⁵ J. H. Kim,⁵ J. Y. Kim,¹ S. B. Kim,⁵ S. Y. Kim,⁷ W. Kim,⁸ E. Kwon,⁵ D. H. Lee,⁷ H. G. Lee,⁷ I. T. Lim,¹ D. H. Moon,¹ M. Y. Pac,² H. Seo,⁷ J. W. Seo,⁵ C. D. Shin,¹ B. S. Yang,⁹ J. Yoo,^{6,9} S. G. Yoon,⁶ I. S. Yeo,³ and I. Yu⁵

(The RENO Collaboration)

¹*Institute for Universe and Elementary Particles, Chonnam National University, Gwangju 61186, Korea*

²*Institute for High Energy Physics, Dongshin University, Naju 58245, Korea*

³*Department of Fire Safety, Seoyeong University, Gwangju 61268, Korea*

⁴*GIST College, Gwangju Institute of Science and Technology, Gwangju 61005, Korea*

⁵*Department of Physics, Sungkyunkwan University, Suwon 16419, Korea*

⁶*Department of Physics, Korea Advanced Institute of Science and Technology, Daejeon 34141, Korea*

⁷*Department of Physics and Astronomy, Seoul National University, Seoul 08826, Korea*

⁸*Department of Physics, Kyungpook National University, Daegu 41566, Korea*

⁹*Institute for Basic Science, Daejeon 34047, Korea*

(Dated: June 5, 2022)

We present a model independent search for sterile neutrino oscillation using 2508.9 days of RENO near detector data and a NEOS published result. The reactor related systematic uncertainties are significantly suppressed as both detectors are located at the same reactor complex of Hanbit Nuclear Power Plant. The search is performed by electron antineutrino ($\bar{\nu}_e$) disappearance between six reactors and two detectors with baselines of 294 m (RENO) and 24 m (NEOS). A spectral comparison of the NEOS prompt-energy spectrum with a prediction from the RENO measurement can explore reactor $\bar{\nu}_e$ oscillations to sterile neutrino. Based on the spectral comparison, we obtain a 90% C.L. excluded region of $10^{-3} < |\Delta m_{41}^2| < 7 \text{ eV}^2$. We also obtain a 68% C.L. allowed region with the best fit of $|\Delta m_{41}^2| = 2.37 \pm 0.03 \text{ eV}^2$ and $\sin^2 2\theta_{14} = 0.09 \pm 0.03$. Comparisons of obtained reactor antineutrino spectra at reactor sources are made among RENO, NEOS and Daya Bay to find a possible spectral variation. The unfolded reactor antineutrino spectra will be useful for studying reactor neutrino physics and particle physics beyond the Standard Model.

PACS numbers: 13.15.+g, 14.60.Pq, 14.60.St, 29.40.Mc

Keywords: sterile neutrino, reactor antineutrino, neutrino oscillation, RENO, NEOS

Precision measurements of the smallest neutrino mixing angle θ_{13} have established the three flavor neutrino (3ν) oscillation framework [1–3]. However, there exist several experimental anomalies that suggest the 3ν model may not be sufficient [4–7]. The existence of additional inactive flavor neutrinos, so-called sterile neutrinos, is often introduced to explain the anomalies.

The RENO and Daya Bay collaborations recently made model independent searches for sterile neutrino oscillations by comparing the observed prompt spectra of near and far detectors and obtained excluded regions of sub-eV sterile neutrino oscillations [8, 9]. The NEOS collaboration reported a result of sterile neutrino search [10] using the Daya Bay’s $\bar{\nu}_e$ spectrum at the reactor [11]. The $\bar{\nu}_e$ spectrum used by NEOS was obtained by including reactor related uncertainties and assuming no sterile neutrino oscillation between reactor and detector. These uncertainties and assumption are not needed if a RENO’s $\bar{\nu}_e$ spectrum is used for the comparison. A spectral comparison of the NEOS prompt spectrum with a prediction from the RENO measurement can explore sterile neutrino oscillations by reactor $\bar{\nu}_e$ disappearance.

This Letter presents a model independent search for sterile neutrino oscillation using 2508.9 days of data taken in the RENO near detector and the published re-

sult based on 180 days of NEOS data [10]. Both detectors are located at the Hanbit Nuclear Power Plant, Yonggwang, Korea. The reactor complex hosts six pressurized water reactors. The maximum thermal output of each reactor is $2.8 \text{ GW}_{\text{th}}$. The RENO near detector is located at 294 m from the center of the reactor array. The NEOS detector is placed in the tendon gallery of the fifth reactor. The distance between the NEOS detector and the reactor core is $23.7 \pm 0.3 \text{ m}$. Both detectors employ gadolinium loaded liquid scintillator to observe the inverse beta decay (IBD) interactions of reactor $\bar{\nu}_e$. Their $\bar{\nu}_e$ target volumes are 16.5 tons for RENO and 0.87 tons for NEOS. Details of RENO and NEOS experiments can be found in Refs. [10, 12, 13].

The combined analysis of RENO and NEOS data removes most of the reactor related uncertainties. Furthermore, a sterile neutrino hypothesis can be tested using the observed spectrum at each baseline, without knowing the $\bar{\nu}_e$ non-oscillation spectrum at reactor. The survival probability of reactor $\bar{\nu}_e$ in the 3+1 ν -oscillation hypothesis is given as [14],

$$P_{\bar{\nu}_e \rightarrow \bar{\nu}_e} = 1 - 4 \sum_{i>j} |U_{ei}|^2 |U_{ej}|^2 \sin^2 \left(\frac{\Delta m_{ij}^2 L}{4E} \right) \simeq 1 - \sin^2 2\theta_{14} \sin^2 \Delta_{41} - \sin^2 2\theta_{13} \sin^2 \Delta_{31}, \quad (1)$$

where $|U_{ei}|$ and $|U_{ej}|$ are the elements of the neutrino mixing matrix, L is the baseline between reactor and detector, E is $\bar{\nu}_e$ energy, $\Delta_{ij} = \Delta m_{ij}^2 L / 4E$, and Δm_{ij} is the mass splitting between the i -th and j -th mass eigenstates. A measured sterile neutrino oscillation probability determines the mixing angle of θ_{14} and the mass squared difference of Δm_{41}^2 . In the region of $\Delta m_{41}^2 \sim 1$ eV², a shorter baseline makes a larger oscillation effect as the reactor $\bar{\nu}_e$ energy is about a few MeV. In the region of larger Δm_{41}^2 ($\gtrsim 3$ eV²), the oscillation effect is averaged out within the volumes of reactor core and detector due to a rapid oscillation and thus hard to be measured by any of existing detectors.

The RENO collaboration has reported an extracted reactor $\bar{\nu}_e$ spectrum [15]. A prompt-energy spectrum at NEOS predicted from the RENO measurement, is obtained using the NEOS detector response function available in Refs. [16, 17]. A comparison in the prompt spectrum between the NEOS measurement and the RENO's prediction is performed in order to find a possible modulation in energy because of a sterile neutrino oscillation. The response function simulates the NEOS detector effects including its energy resolution. There exists somewhat difference between RENO and NEOS in detecting IBD candidate events. A small volume of the NEOS detector without a gamma-catcher surrounding its target allows escape of γ -rays and causes no single gaussian energy response to a monochromatic gamma-ray source [16, 17]. Therefore, a careful check is required to ensure that the detector response function reproduces the full NEOS detector effects. A prompt spectrum is obtained by convoluting the detector response into the reactor $\bar{\nu}_e$ spectrum of the Huber and Mueller (HM) model [18, 19] and compared with the NEOS Monte Carlo (MC) prediction. The agreement is found to be within 0.5%, corresponding to 2.3% of the total spectral-shape uncertainty, for 1 to 7 MeV of prompt energy range.

Using the detector response function, a $\bar{\nu}_e$ spectrum is extracted by unfolding the NEOS observed prompt spectrum, and compared with that of RENO. This provides a direct comparison of their reactor $\bar{\nu}_e$ spectra as well as another systematic check of the NEOS response function relative to its full detector MC simulation. A covariance matrix used by the unfolding is constructed from the uncertainties in Ref [10]. The largest contribution to the matrix elements comes from the energy scale uncertainty. The energy bin-by-bin correlation in the prompt spectrum is estimated by randomly shifting the energy scale by $\pm 0.5\%$ using a toy MC.

The detector response effects in the NEOS prompt spectrum are removed by an unfolding method of Iterative Bayesian Unfolding (IBU) [20]. The systematic uncertainties are included through the covariance matrix. The IBU is relatively insensitive to the initial input of a true spectrum compared to other methods. The RooUnfold package [21] is used to implement the IBU algorithm.

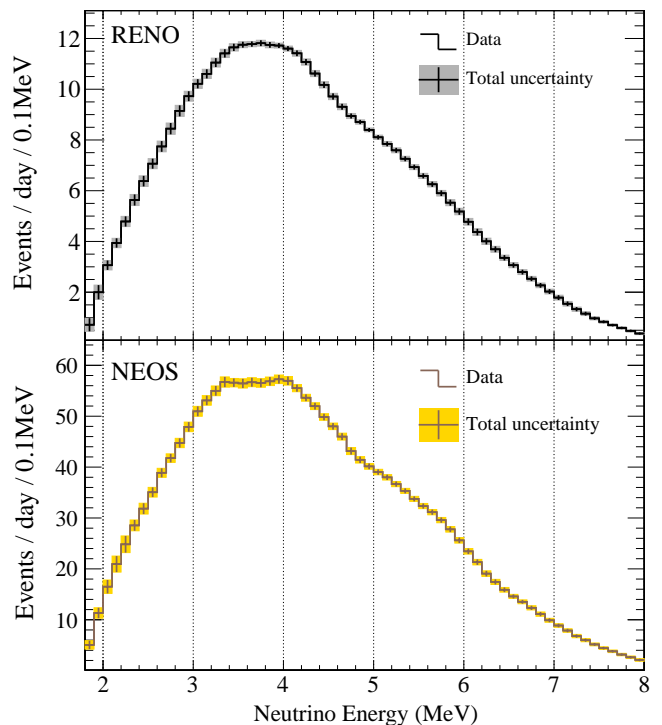


FIG. 1. Reactor antineutrino spectra obtained from the measured IBD prompt spectra of RENO and NEOS after unfolding their detector effects. The shaded boxes represent total uncertainties in the corresponding energy bins.

The total fluctuation and the residual uncertainty are minimized at 5-th iteration which is determined by the L-curve criterion [22]. Since the NEOS prompt spectrum below 1 MeV is unavailable in Ref. [10], the HM predicted spectrum is used in that energy range. The unfolding uncertainty for the NEOS $\bar{\nu}_e$ spectrum is estimated to be 0.5% by varying the number of iterations. Details of the unfolding process can be found in Ref. [15] and the references there in.

Figure 1 shows the extracted RENO and NEOS $\bar{\nu}_e$ spectra with detector effects unfolded. The uncertainties of reactor thermal power and detection efficiencies are irrelevant to the shape of the spectrum and not included in this analysis. Table I lists the fractional errors

TABLE I. Fractional errors in the RENO and NEOS $\bar{\nu}_e$ spectra between 2.2 and 7.0 MeV.

| Error component | RENO (%) | NEOS (%) |
|----------------------------|----------|----------|
| Energy scale | 1.8 | 1.0 |
| Statistical | 0.8 | 1.6 |
| Unfolding | 0.3 | 0.5 |
| Background | 0.3 | 0.4 |
| NEOS response reproduction | - | 0.5 |
| Total | 2.0 | 2.1 |

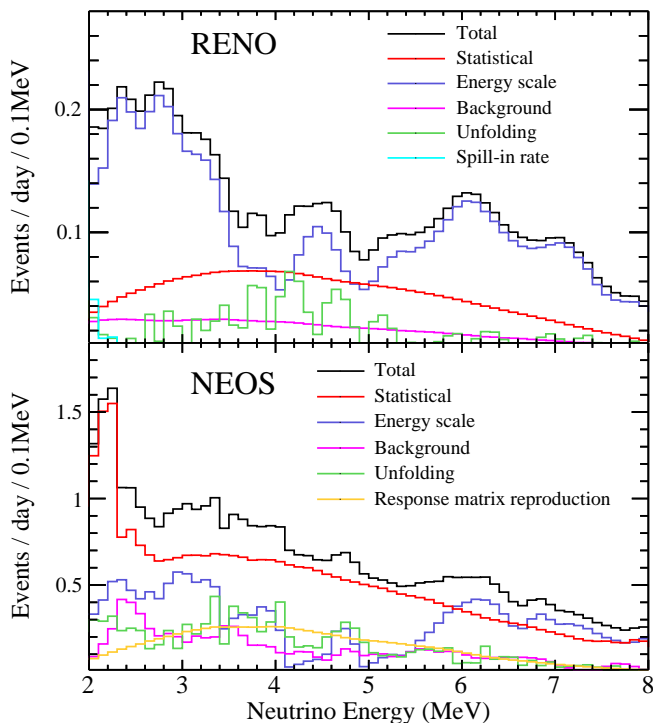


FIG. 2. Uncertainties of unfolded RENO and NEOS $\bar{\nu}_e$ spectra.

of RENO and NEOS $\bar{\nu}_e$ spectra in the energy range between 2.2 and 7.0 MeV. The errors due to various uncertainty sources are shown as a function of $\bar{\nu}_e$ energy in Fig. 2. The error of neutrino energy less than 2.4 MeV mostly comes from use of the HM predicted spectrum below prompt energy 1 MeV.

The extracted $\bar{\nu}_e$ spectra are corrected for different fuel isotope fractions between RENO and NEOS due to their mismatched data-taking periods. The correction is made using the HM predicted spectra [18, 19]. The average fission fractions of ^{235}U , ^{238}U , ^{239}Pu , and ^{241}Pu are 0.571 (0.655), 0.073 (0.072), 0.300 (0.235), and 0.056 (0.038), respectively, for RENO (NEOS). Using the well-understood response function, the RENO's expected prompt spectrum at NEOS is obtained from the 3ν best-fit predicted $\bar{\nu}_e$ spectrum from the RENO measurement. The upper panel of Fig. 3 shows the RENO prediction at NEOS divided by the NEOS observed prompt spectrum. The NEOS measured absolute $\bar{\nu}_e$ flux is not available and thus normalized to that of RENO measurement, for a spectral shape comparison only. Also shown in the lower panel of Fig. 3 is the ratio of the RENO prediction at NEOS relative to the NEOS extracted $\bar{\nu}_e$ spectrum. In the spectral comparisons, the uncertainties are assumed to be fully uncorrelated between the RENO and NEOS spectra.

A method of $\Delta\chi^2$ is used for this sterile neutrino

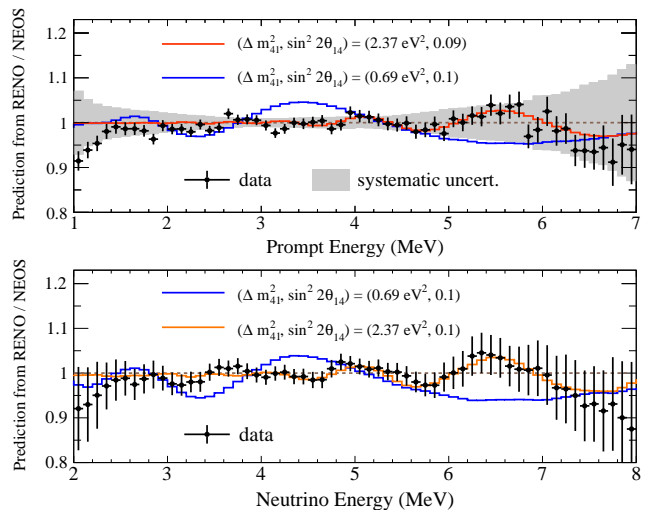


FIG. 3. Upper: Ratio of the RENO prediction at NEOS relative to the NEOS observed prompt spectrum. The error bars represent the statistical uncertainty only. The areas of two spectra are normalized for a shape comparison. The gray band indicates the systematic uncertainty. Lower: Ratio of the RENO prediction at NEOS relative to the NEOS extracted $\bar{\nu}_e$ spectrum. The error bars represent the statistical and systematic uncertainties. The orange curves in the both panels represent the best fits to the data. The blue curves represent spectral ratios expected with one of sterile neutrino oscillation parameters that are excluded by this analysis.

search. A χ^2 function is constructed as,

$$\chi^2 = \sum_{i,j}^N \left(N_{\text{R}}^i - \alpha \frac{M_{\text{R}}^i}{M_{\text{N}}^i} N_{\text{N}}^i \right) V_{ij}^{-1} \left(N_{\text{R}}^j - \alpha \frac{M_{\text{R}}^j}{M_{\text{N}}^j} N_{\text{N}}^j \right), \quad (2)$$

where N_{R}^i and N_{N}^i are the numbers of observed events in the i -th $\bar{\nu}_e$ energy bin at RENO and NEOS, respectively, M_{R}^i and M_{N}^i are the numbers of events expected from sterile neutrino oscillation parameters, α is a scale factor for the shape comparison, and V_{ij} is a covariance matrix element for a total spectral error of RENO and NEOS in the i -th and j -th $\bar{\nu}_e$ energy cell. The matrix element is given by,

$$V_{ij} = V_{\text{R}}^{ij} + \alpha^2 \left(\frac{M_{\text{R}}^i}{M_{\text{N}}^i} \right) \cdot \left(\frac{M_{\text{R}}^j}{M_{\text{N}}^j} \right) V_{\text{N}}^{ij}, \quad (3)$$

where V_{R}^{ij} and V_{N}^{ij} are covariance matrix elements of RENO and NEOS, respectively. The value of minimum χ^2/NDF for the RENO measured 3ν oscillation parameters is 34.9/59 where NDF is the number of degrees of freedom. The value for the sterile neutrino oscillation is 23.2/57. The best fit shown in Fig. 3 is found at $|\Delta m_{41}^2| = 2.37 \text{ eV}^2$ and $\sin^2 2\theta_{14} = 0.09$. The spectral ratio of data appears to be consistent with the best-fit expectation including the energy modulation. Because of its large systematic uncertainty, the value of $\Delta\chi^2 = \chi_{3\nu}^2 - \chi_{4\nu,\text{min}}^2$ is 11.7 corresponding to the p-value of 0.13, and thus shows no significant indication of a sterile neutrino oscillation.

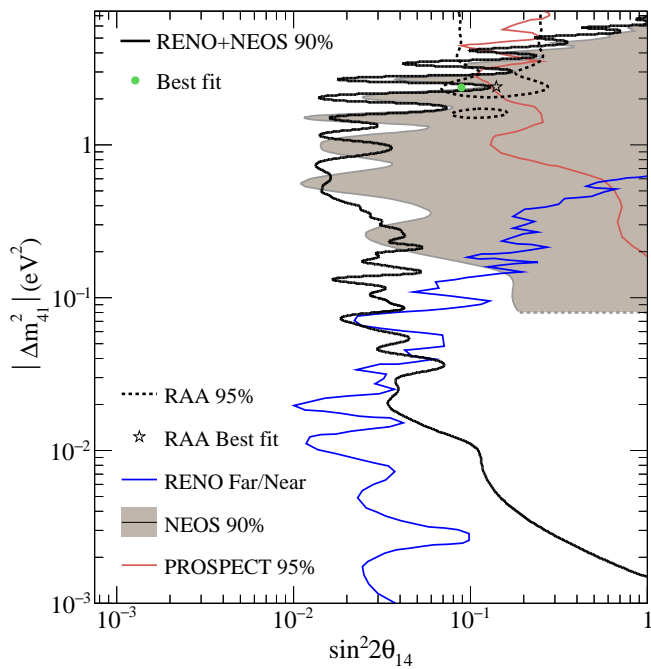


FIG. 4. Comparison of the exclusion limits on sterile neutrino oscillations and an allowed region. The right side of each contour indicates an excluded region. The black thick curve represents a 90% C.L. exclusion contour obtained from the RENO and NEOS combined search. The best fit parameter (green circle) is found at $|\Delta m_{41}^2| = 2.37 \text{ eV}^2$ and $\sin^2 2\theta_{14} = 0.09$. For the comparison, the NEOS [10] 90% C.L. (gray shaded), Bugey-3 [23] 90% C.L. (blue), PROSPECT [24] 95% C.L. (red), and RENO [8] 95% C.L. (gray) limits on the disappearance are shown. Also shown is a 95% C.L. allowed region of RAA [25] (black dotted) with the best fit [26] (star) at $|\Delta m_{41}^2| = 2.4 \text{ eV}^2$ and $\sin^2 2\theta_{14} = 0.14$.

A method of raster scan [10, 27] is used to obtain exclusion limits on sterile neutrino oscillation parameters. For each set of $\sin^2 2\theta_{14}$ and $|\Delta m_{41}^2|$, $\Delta\chi^2 = \chi^2 - \chi_{min}^2$ is calculated where χ_{min}^2 is the minimum χ^2 . The parameter sets of $\sin^2 2\theta_{14}$ and $|\Delta m_{41}^2|$ are excluded at 90% confidence level if $\Delta\chi^2$ is greater than 2.71 [27]. Figure 4 shows exclusion contours obtained from the RENO and NEOS data and other search results. It also shows a 95% C.L. allowed region of reactor antineutrino anomaly (RAA) [25]. The sensitive search region is enlarged from the NEOS result [10]. This improvement is given by the spectral comparison based on the RENO $\bar{\nu}_e$ spectrum at the same reactor complex. The reduced systematic uncertainty associated with reactors allows additionally excluded $\sin^2 2\theta_{14}$ parameters. The extended sensitivity in the $|\Delta m_{41}^2| < 0.1 \text{ eV}^2$ region comes from the longer baseline of the RENO near detector than NEOS. Note that the NEOS search result [10] was based on the Daya Bay's $\bar{\nu}_e$ spectrum obtained at reactor by assuming no sterile neutrino oscillation between reactor and detector [11]. A search is repeated with the extracted $\bar{\nu}_e$ spectra of RENO

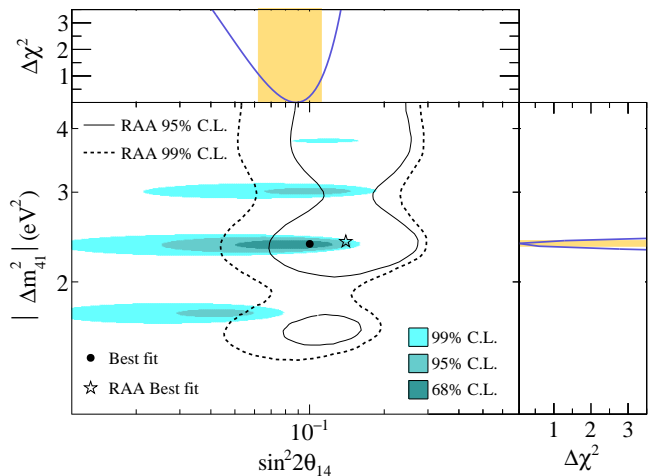


FIG. 5. Allowed regions of 68%, 95%, and 99% C.L. obtained from the RENO and NEOS observed prompt-energy spectra compared with those obtained from RAA [25]. The best fit values are given by the filled circle, and the RAA best fit values by the star. The $\Delta\chi^2$ distributions for $\sin^2 2\theta_{14}$ (top) and $|\Delta m_{41}^2|$ (right) are also shown with an 1σ band.

and NEOS as shown in the lower panel of Fig. 3 and obtains a similar excluded contour.

As the RENO and NEOS data appear to be consistent with the best-fit prediction within their uncertainties in Fig. 3, the $\Delta\chi^2$ analysis is again performed to obtain allowed parameters. Figure 5 shows 68%, 95%, and 99% C.L. allowed regions obtained from the RENO and NEOS data and the allowed region of RAA by Ref. [25]. The best fit is found at $|\Delta m_{41}^2| = 2.37 \pm 0.03 \text{ eV}^2$ and $\sin^2 2\theta_{14} = 0.09 \pm 0.03$, whereas that of RAA at $|\Delta m_{41}^2| = 2.4 \text{ eV}^2$ and $\sin^2 2\theta_{14} = 0.14$ [26]. They are consistent with each other at 1.7σ confidence level because of their χ^2 difference of 4.9. An improved measurement of reactor $\bar{\nu}_e$ flux and energy spectrum with a substantially reduced systematic uncertainty is essential to obtain a conclusive result on sterile neutrino oscillation.

The extracted $\bar{\nu}_e$ spectra of RENO, NEOS and Daya Bay are corrected for their different fuel isotope fractions and converted to the 3ν non-oscillating spectra at reactor using the global best-fit parameters [14]. Figure 6 shows spectral shape comparisons exhibiting interesting discrepancies among them. The reactor related uncertainty is negligible in the spectral comparison between RENO and NEOS because of their common reactor complex, and estimated to be around 0.3% between Daya Bay and one of the other two. While the discrepancy between RENO and Daya Bay is observed mostly between 2 and 3 MeV and minimal at the rest of energies, the comparison between RENO and NEOS shows a spectral modulation consistent with the expectation from the best fit as shown in Fig. 3. The spectral comparison between Daya Bay and NEOS also shows a quite similar modulation in energy. Because of the minimal difference

between RENO and Daya Bay, the modulation possibly comes from the NEOS obtained $\bar{\nu}_e$ spectrum as a result of an unknown uncertainty in the measurement or sterile neutrino oscillations. Significant improvement of systematic uncertainties is required for complete understanding of the observed differences in the $\bar{\nu}_e$ spectra.

In summary, we report a model independent search for sterile neutrinos using data from the RENO near detector and the NEOS detector. As the RENO and the NEOS detectors share the same reactor complex, this analysis removes the $\bar{\nu}_e$ source dependency in the previous NEOS sterile neutrino search [10]. This analysis uses IBD spectra measured at RENO and NEOS detector locations without knowing a non-oscillation spectrum at reactor. Based on the spectral comparison of the NEOS prompt-energy spectrum with a prediction from the RENO measurement, we obtain a 90% C.L. excluded region of $10^{-3} < |\Delta m_{41}^2| < 7 \text{ eV}^2$. We also obtain an allowed region with the best fit of $|\Delta m_{41}^2| = 2.37 \pm 0.03 \text{ eV}^2$ and $\sin^2 2\theta_{14} = 0.09 \pm 0.03$. The results set the stringent constraints in the $0.1 < |\Delta m_{41}^2| < 7 \text{ eV}^2$ range. Comparisons of obtained reactor antineutrino spectra at reactor sources are made among RENO, NEOS and Daya Bay and show an interesting spectral variation within their systematic uncertainties. The model independent reactor neutrino spectra in this report will be useful studying reactor neutrino physics and particle physics beyond the Standard Model.

The RENO experiment is supported by the National Research Foundation of Korea (NRF) grants No. 2009-0083526, No. 2019R1A2C3004955, and 2017R1A2B4011200 funded by the Korea Ministry of Science and ICT. Some of us have been supported by a fund from the BK21 of NRF and Institute for Basic Science (IBS-R017-D1-2020-a00/IBS-R017-G1-2020-a00). We gratefully acknowledge the cooperation of the Hanbit Nuclear Power Site and the Korea Hydro & Nuclear Power Co., Ltd. (KHNP). We thank KISTI for providing computing and network resources through GSDC, and all the technical and administrative people who greatly helped in making this experiment possible

-
- [1] J. Ahn *et al.* (RENO), Phys. Rev. Lett. **108**, 191802 (2012), arXiv:1204.0626 [hep-ex].
 - [2] F. An *et al.* (Daya Bay), Phys. Rev. Lett. **108**, 171803 (2012), arXiv:1203.1669 [hep-ex].
 - [3] Y. Abe *et al.* (Double Chooz), Phys. Rev. Lett. **108**, 131801 (2012), arXiv:1112.6353 [hep-ex].
 - [4] C. Athanassopoulos *et al.* (LSND), Phys. Rev. Lett. **77**, 3082 (1996), arXiv:nucl-ex/9605003.
 - [5] A. Aguilar-Arevalo *et al.* (MiniBooNE), Phys. Rev. Lett. **110**, 161801 (2013), arXiv:1303.2588 [hep-ex].
 - [6] W. Hampel *et al.* (GALLEX), Phys. Lett. B **447**, 127

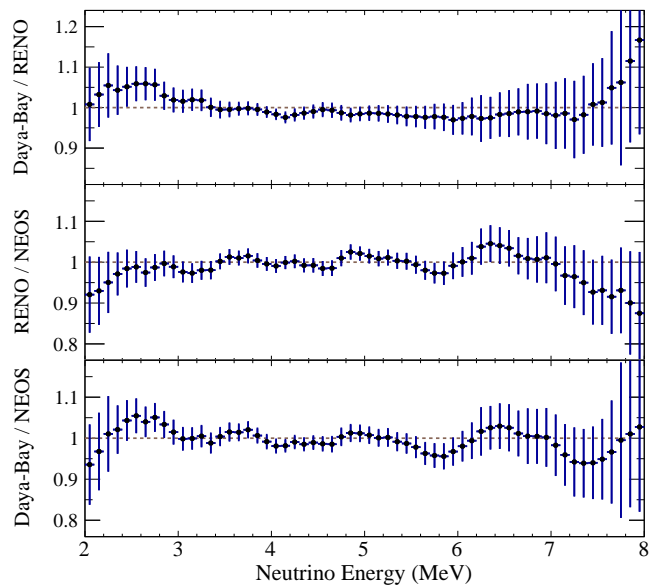


FIG. 6. Comparisons of 3ν non-oscillating $\bar{\nu}_e$ spectra at reactor source among RENO, NEOS and Daya Bay. The differences of fission fractions are corrected. Statistical uncertainties and systematic uncertainties are combined and represented as the error bars. Note that the reactor related uncertainty is not included in the errors of RENO/NEOS, while Daya-Bay/RENO and Daya-Bay/NEOS include reactor uncertainty.

- (1999).
- [7] J. Abdurashitov *et al.* (SAGE), Phys. Rev. C **60**, 055801 (1999), arXiv:astro-ph/9907113.
- [8] J. Choi *et al.* (RENO), (2020), arXiv:2006.07782 [hep-ex].
- [9] P. Adamson *et al.* (MINOS+, Daya Bay), Phys. Rev. Lett. **125**, 071801 (2020), arXiv:2002.00301 [hep-ex].
- [10] Y. Ko *et al.* (NEOS), Phys. Rev. Lett. **118**, 121802 (2017), arXiv:1610.05134 [hep-ex].
- [11] F. P. An *et al.* (Daya Bay), Chin. Phys. C **41**, 013002 (2017), arXiv:1607.05378 [hep-ex].
- [12] S. H. Seo *et al.* (RENO), Phys. Rev. **D98**, 012002 (2018), arXiv:1610.04326 [hep-ex].
- [13] J. K. Ahn *et al.* (RENO), Technical Design Report (2010), arXiv:1003.1391 [hep-ex].
- [14] P. A. Zyla *et al.* (Particle Data Group), Progress of Theoretical and Experimental Physics **2020** (2020).
- [15] Z. Atif *et al.* (RENO), arXiv:2010.14989 [hep-ex].
- [16] Y. Oh (NEOS), in *39th ISNP* (2017).
- [17] H. Kim (NEOS), in *13th Rencontres du Vietnam: Neutrinos 2017* (2017).
- [18] P. Huber, Phys. Rev. C **84**, 024617 (2011).
- [19] T. A. Mueller, D. Lhuillier, M. Fallot, A. Letourneau, S. Cormon, M. Fechner, L. Giot, T. Lasserre, J. Martino, G. Mention, A. Porta, and F. Yermia, Phys. Rev. C **83**, 054615 (2011).
- [20] G. D'Agostini, Nuclear Instruments and Methods in Physics Research Section A: Accelerators, Spectrometers, Detectors and Associated Equipment **362**, 487 (1995).
- [21] T. Adye, in *Proceedings, PHYSTAT 2011 Workshop on Statistical Issues Related to Discovery Claims in Search*

- Experiments and Unfolding, CERN, Geneva, Switzerland 17-20 January 2011* (CERN, Geneva, 2011) pp. 313–318, arXiv:1105.1160 [physics.data-an].
- [22] C. L. Lawson and R. J. Hanson, *Solving least squares problems*, Classics in Applied Mathematics, Vol. 15 (Society for Industrial and Applied Mathematics (SIAM), Philadelphia, PA, 1995) pp. xii+337, revised reprint of the 1974 original.
- [23] Y. Declais *et al.*, Nucl. Phys. B **434**, 503 (1995).
- [24] J. Ashenfelter *et al.* (PROSPECT), Phys. Rev. Lett. **121**, 251802 (2018), arXiv:1806.02784 [hep-ex].
- [25] G. Mention, M. Fechner, T. Lasserre, T. Mueller, D. Lhuillier, M. Cribier, and A. Letourneau, Phys. Rev. D **83**, 073006 (2011), arXiv:1101.2755 [hep-ex].
- [26] K. Abazajian *et al.*, (2012), arXiv:1204.5379 [hep-ph].
- [27] L. Lyons, (2014), arXiv:1404.7395 [hep-ex].